POLITECNICO DI TORINO
Repository ISTITUZIONALE

Glyphosate adsorption performances of polymer-derived SiC/C aerogels

Original
Glyphosate adsorption performances of polymer-derived SiC/C aerogels / Zambotti, Andrea; Bruni, Angela; Biesuz, Mattia; Sorarù, Gian Domenico; Rivoira, Luca; Castiglioni, Michele; Onida, Barbara; Bruzzoniti, Maria Concetta. - In: JOURNAL OF ENVIRONMENTAL CHEMICAL ENGINEERING. - ISSN 2213-3437. - 11:3(2023), p. 109771. [10.1016/j.jece.2023.109771]

Availability:
This version is available at: 11583/2977989 since: 2023-04-20T10:09:37Z

Publisher:
Elsevier

Published
DOI:10.1016/j.jece.2023.109771

Terms of use:

This article is made available under terms and conditions as specified in the corresponding bibliographic description in the repository

Publisher copyright
Elsevier postprint/Author's Accepted Manuscript

© 2023. This manuscript version is made available under the CC-BY-NC-ND 4.0 license
http://creativecommons.org/licenses/by-nc-nd/4.0/.The final authenticated version is available online at:
http://dx.doi.org/10.1016/j.jece.2023.109771

(Article begins on next page)

06 May 2026

Glyphosate adsorption performances of polymer-derived SiC/C aerogels

Andrea Zambotti*[1,2], Angela Bruni[1], Mattia Biesuz[1], Gian Domenico Sorarù[1], Luca Rivoira[3], Michele Castiglioni[3], Barbara Onida[4], Maria Concetta Bruzzoniti*[3]

[1] Department of Industrial Engineering, University of Trento, Via Sommarive 9, 38123 Trento, Italy

[2] Technische Universität Darmstadt, Institut für Materialwissenschaft, Petersenstrasse 23, D-64287 Darmstadt, Germany

[3] Department of Chemistry, University of Torino, Via Pietro Giuria 7, 10125, Torino, Italy

[4] Department of Applied Science and Technology, Polytechnic of Turin, Corso Duca degli Abruzzi 24, 10129 Turin, Italy

* Corresponding authors: andrea.zambotti-1@unitn.it; mariaconcetta.bruzzoniti@unito.it

Abstract

The phenomenon of water pollution as a consequence of the release of herbicides and pesticides into the environment is an outgrowing problem that requires performing and regenerable adsorbent materials. This work presents the synthesis of a nanocrystalline silicon carbide aerogel and its application in removing glyphosate from polluted water. The aerogel was synthesized via Polymer-Derived Ceramic (PDC) route using allylhydridopolycarbosilane as polymeric precursor. By pyrolysis at 1500°C in argon, the crystallization of *β*-SiC nanocrystals was observed, while the aerogel preserved a high specific surface area of 215 $m^2 \cdot g^{-1}$. The nanostructured aerogel was tested for glyphosate herbicide, showing a remarkable adsorption of 0.607 $mg \cdot g^{-1}$, being the initial glyphosate concentration of 2 $mg \cdot L^{-1}$, and a removal of 93% of the pollutant in solution. Elovich kinetics adsorption and Langmuir isotherm models were found to be the most suitable to describe the mechanism of glyphosate capture via adsorption onto the aerogel surface.

Keywords: Glyphosate, Polymer-Derived Ceramics, Water purification, Silicon Carbide, Aerogel

1. Introduction

As the human population keeps growing worldwide, the use of pesticides to sustain the food demand rises as well, and it is expected to increase of two times in the next 30 years, from 5 to 10 billions kilograms per year [1]. The indiscriminate use and disposal of pesticides and their agricultural persistence in the soil and water are a dangerous combination of factors that bring hazardous substances under the spotlight of serious environmental and health threats. Besides the functional toxicity of pesticides, the lack of a proper knowledge on their handling and use represents both a risk not only for direct users but also for living organisms that are fundamental for biodiversity and to the most disparate life-cycles. In fact, the spread of these hazardous substances must be tightly controlled to also prevent any further poisoning of food chains, posing a serious threat to millions of people [2]. As the use of pesticides keeps growing, many studies have been conducted to asses any correlation with the incidence of certain types of diseases, including cancers, revealing clear exposure-response relations in the case of several pesticides [3,4]. Therefore, many countries have imposed maximum residue limits (MRLs) of pesticides in foods. As a matter of fact, while some pesticides result harmless as a consequence of biodegradability (e.g., phosphates and inorganic salts), others can persist in the environment for years [5]. In particular, glyphosate can penetrate the soil and bound to its organic and mineral components, losing its herbicide potential [6]. However, it is known that even though glyphosate can tightly bind to common oxides present in the soil (e.g., iron and aluminium oxides), its desorption from organic humus is way faster, with the consequence of a reintroduction of the herbicide in the environment.

In the framework of ground- and wastewater purification, a growing attention has been drawn to glyphosate and potential sorbents for its removal [7,8]. Among these, activated carbons are typically recognized as performing and versatile sorbents thanks to the characteristic microporosity and very high surface area [9].

However, there are also other routes for producing ultra-porous materials, such as the polymer-derived ceramic (PDC) route, which mainly employs silicon-based polymers for the synthesis of advanced ceramics systems such as SiOC, SiCN SiCBN via molecular approach. Owing to the versatility of this chemical route in functionalizing Si-based polymers to achieve the most disparate complex systems, the PDC route also allows obtaining ceramic components with complex shapes and nanometric microstructures [10]. Among them, polymer-derived ceramic aerogels are obtained via crosslinking and supercritical drying of preceramic gels,

showing high porosity and specific surface area after the ceramization process [11]. Owing to these properties and their tailored chemistry, PDC aerogels found applications in energy and environmental applications, as shape-stabilizers for thermal energy storage[12,13], catalyst supports [14] and as battery electrodes [15]. Moreover, polymer-derived ceramic (PDC) aerogels and foams have also been reported as excellent porous sorbent for water contaminated with organic compounds (dyes) or non-steroidal anti-inflammatory drugs [16–18]; as well as heavy metals [19]. Inspired by the abovementioned results, in this paper we aim at exploiting this type of porous solids, namely PDC aerogels of the SiC-C system, as ultra-porous sorbents for glyphosate capture trying to assess and identify the sorption mechanisms together with the characterization of the performances of such material.

2. Experimental

2.1 Synthesis method

Allylhydropolycarbosilane StarPCS™ SMP-10 was purchased from Starfire Systems (Schenectady, NY, USA), while divinylbenzene (DVB, CAS: 1321-74-0) and platinum Karstedt's catalyst (CAS: 68478-92-2) from Sigma Aldrich. Cyclohexane (Carlo Erba, CAS: 110-82-7) was used as synthesis solvent. For the synthesis, a weight ratio of 1:2.58 between SMP-10 and DVB was selected, as it roughly corresponds to a 1:1 molar ratio between Si-H and DVB vinyl groups and the crosslinking reaction occurs via hydrosilylation between the Si-H moieties of the polycarbosilane and the vinyl groups of DVB [20]. In order to guarantee a good mixing of the two reagents and to plan the synthesis of a highly porous aerogel, the cyclohexane volume fraction of the overall mixture was fixed to 80%. Finally, 100 µl of diluted Pt catalyst (0.2% in Xylene) per gram of utilized SMP-10 were added to the mixture, while stirring it for 5 minutes at room temperature.

The crosslinking reaction between SMP-10 and DVB was performed at 150°C for 5h in a sealed digestion vessel (Parr Instruments model 4749, Moline, IL, USA), in such a way that no cyclohexane could evaporate. The vessel was loaded of at least two-thirds of its internal volume. After gelification, the so-obtained wet gel was subjected to 6 washings in fresh cyclohexane (two per day) to eliminate unreacted species, and then dried

in supercritical conditions after proceeding with a solvent exchange between cyclohexane and liquid carbon dioxide. This intermediate step was characterized by six interdiffusive exchanges with fresh CO_2 (two per day) at 10°C in a customized autoclave.

After supercritical drying, the preceramic aerogel was pyrolyzed in argon at 1000°C or 1500°C for one hour, with a heating/cooling rate of 5 °C·min^{-1}, resulting in the formation of a SiC/C polymer-derived ceramic aerogel. These two temperatures were selected to compare the glyphosate retention ability of amorphous and crystalline SiC, respectively, as crystallization starts around 1200°C [21,22]. Samples were labelled according to their composition (SMP-10 plus DVB) and pyrolysis temperature: 1:1SD 1000°C and 1:1 SD 1500°C.

2.2 Characterization and performances measurements

Fourier-Transform Infrared Spectroscopy (FT-IR) was adopted as characterization method for the definition of chemical bonds both in the preceramic and ceramic aerogels. A Nicolet Avatar 330 FT-IR spectrophotometer (Thermo Fischer Scientific, Waltham, MA, USA) was employed in transmission mode with KBr pellets in the 4000-400 cm^{-1} wavenumber range. A total of 64 scans per spectrum were acquired, imposing a resolution of 4 cm^{-1}.

Nitrogen physisorption isotherms were acquired at 77.35 K with a Autosorb iQ analyzer (Anton Paar, Gratz, AU). The multipoint Brunauer-Emmett-Teller (BET) theory was adopted for the calculation of the specific surface area (SSA), while Non-Local Density Functional Theory (NLDFT) was employed on the adsorption branch as computational method for the definition of pore size distributions in the micro-mesopore range of the polymer-derived aerogels. Silica with cylindrical pores was selected as model material for these calculations.

Micrographs of the ceramic aerogel morphology were acquired with a Carl Zeiss Gemini SUPRA 40 Scanning Electron Microscope equipped with a field emission gun (FE-SEM).

X-ray diffraction (XRD) was performed with a Italstructures IPD 3000/CPD120 instrument, featuring a 2000 W cobalt source coupled with an incident beam multilayer monochromator and a Inel CPS 120 detector (5°-125° range, 4095 channels).

For what concerns the oxidative thermogravimetric analysis (TGA), a Netzsch STA 409 Thermobalance was used. The analysis was conducted under pure flowing air (100 $cm^3 \cdot min^{-1}$) with a heating rate of 5°C·min^{-1} in the 20-1500°C temperature range.

2.3 Adsorption performances

Preliminary adsorption tests with 17.5 mL of 2 mg·L^{-1} glyphosate (Sigma Aldrich), pH 6.2 were performed on 0.1 g of aerogel pyrolyzed both at 1000°C and 1500 °C (time of contact 48h). Insight studies on adsorption kinetics and isotherms (sections 2.3.1. and 2.3.2) were accomplished with the best performing ceramic aerogel (i.e. aerogel obtained at 1500 °C) .

2.3.1 Adsorption kinetics

Batch experiments were performed in triplicate using 0.025 g of ceramic aerogel (1500 °C) in contact with 17.5 mL of 2 mg·L^{-1} glyphosate , pH 6.2, for defined period of times. A blank was run in parallel. The initial glyphosate concentration, being representative of medium-high level environmental contamination, was chosen to allow a reliable determination of the residual glyphosate remained in the solution after adsorption.

Samples were withdrawn at fixed time intervals (0.5, 1, 2, 4, 8, 24 and 48 h), filtered with 0.22 µm nylon filters and injected in an ion chromatograph (ICS-3000 Thermo Fisher, Dionex, CA, USA) for the analysis of the residual concentration of glyphosate in the solution (C_e, mg L^{-1}). For this purpose, an anion-exchange column IonPac AS16 4x250 mm (Thermo Fisher, Dionex, CA, USA) was used with a mobile phase 18 mM NaOH (0.25 mL·min^{-1} flow rate); a suppressed conductivity detection was employed.

2.3.2 Adsorption isotherms

Triplicate experiments were performed with 2 mg·$L^{-1}$of glyphosate (17 mL solution, pH 6.2) using different weights of ceramic aerogels (1500 °C) in the range 0.005-0.05 g. Samples containing glyphosate and ceramic aerogel were stirred at room temperature for 24 h (after verifying that the equilibrium conditions were achieved according to adsorption kinetics). The range of the aerogel amount explored allowed reliable determination of glyphosate remained in the solution after adsorption. A control was processed in parallel.

The amount of glyphosate adsorbed at equilibrium (q_e in mg·g^{-1}) was determined as follows:

$$q_e = \frac{(C_0 - C_e) \cdot V}{m} \quad (1)$$

where V (L) is the volume of solution, m (g) is the mass of the adsorbent, and C_0 (mg·L^{-1}) is the initial concentration of the analyte (in mg·L^{-1}).

The percentage of glyphosate absorbed (R_{ads}) was calculated as follows:

$$R_{ads} = \frac{C_0 - C_e}{C_0} \cdot 100 \quad (2)$$

3. Results and Discussion

3.1 Features of the polymer-derived aerogel

The preceramic aerogel was characterized by means of FT-IR spectroscopy and N_2 physisorption to assess the main chemical and microstructural features prior to the ceramization process. The FT-IR spectrum reported in **Figure 1a** visualizes the chemical bonds present in the crosslinked aerogel, which consist in the superimposition of those of the allylhydropolycarbosilane and divinylbenzene. The main peaks assigned to the polycarbosilane are hereby reported: δ Si-CH_3 at 763 cm^{-1}, δ Si-C at 839, ν Si-H at 952 cm^{-1} and 2141 cm^{-1}, Si-CH_2-Si at 1049 cm^{-1}, respectively [23]. The organic groups of the polycarbosilane are clearly visible around 3000 cm^{-1}. Unassigned peaks are relative to organic species belonging to the divinylbenzene crosslinker. Since silyl bonds at 2141 and 952 cm^{-1} can still be observed in the preceramic FT-IR spectrum of the aerogel, it is clear that a certain fraction of Si-H moieties did not take part in the hydrosilylation reaction that formed the gel [24]. However, it is reasonable that both steric hindrance and vinyl-vinyl reactions might have a role in decreasing the efficiency of hydrosilylation. Besides, it is worth underlying that the effective chemical structure of SMP-10 is rather difficult to assess due to the unknown degree of branching of the neat polymer itself, so that the nominal molar ratio between Si-H and DVB vinyl groups is tentatively estimated considering

no branching of the polycarbosilane, i.e. by considering the following formula: $–[SiH_2–CH_2]_x–[SiH(allyl)–CH_2]_y–$, where x:y = 9:1.

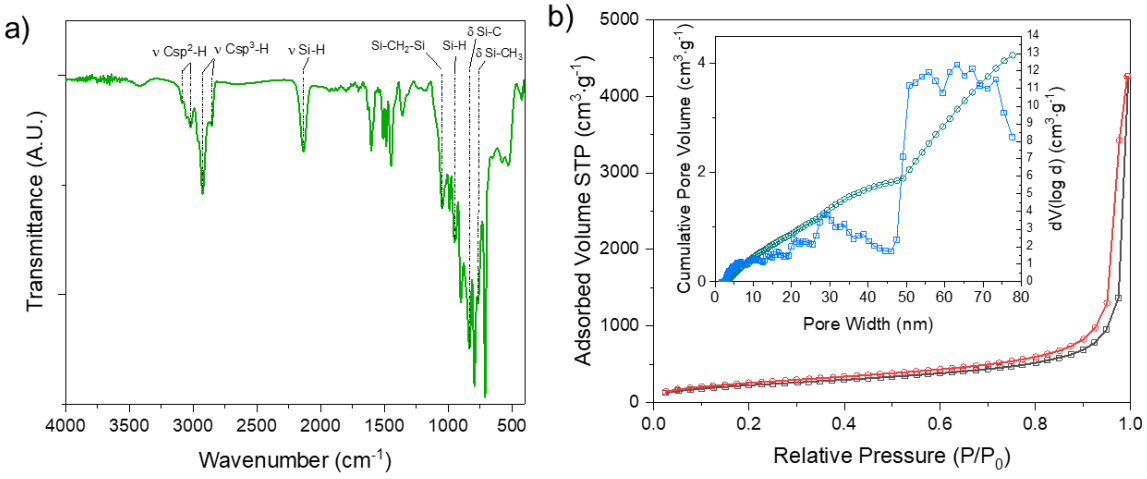

Figure 1: a) Infrared spectrum of the preceramic aerogel, acquired in transmission; b) N_2 Adsorption/desorption isotherm and DFT pore volume distribution (inset) of the preceramic aerogel.

The nitrogen physisorption analysis reported in **Figure 1b** shows the adsorption/desorption isotherm and the pore volume distribution (inset) of the preceramic aerogel. Multipoint BET calculation allows to define a specific surface area of 834 $m^2 \cdot g^{-1}$, which is distributed in what could be defined as a bimodal meso-macroporous structure, as depicted by the DFT pore volume distribution in **Figure 1b**. As a matter of fact, half of the cumulative pore volume of 4.2 $cm^3 \cdot g^{-1}$ is found in the mesopore range (i.e., 2-50 nm), while the other half is given by pores with a diameter greater than 50 nm. This information gives an explanation to the shape of the isotherm in **Figure 1b**. According to the IUPAC classification, it presents a Type II shape, typical of macroporous sorbents, but with an hysteresis loop given by capillary condensation of N_2 in mesopores near the saturation point [25].

Subsequently to the pyrolysis at 1500°C in argon, the FT-IR spectrum of ceramic aerogel (**Figure 2**) presents a broad peak between 770 and 950 cm^{-1}, which is representative of the optical absorption region of the crystalline lattice of SiC [26,27]. Finally, the absorption shoulder at 1590 cm^{-1} is attributed to C=C bonds of the free carbon phase [28]. For comparison, in **Figure 2** we report also the spectrum of the same sample

pyrolyzed at 1000°C, which do not present any significant absorption in the abovementioned Si-C vibration range.

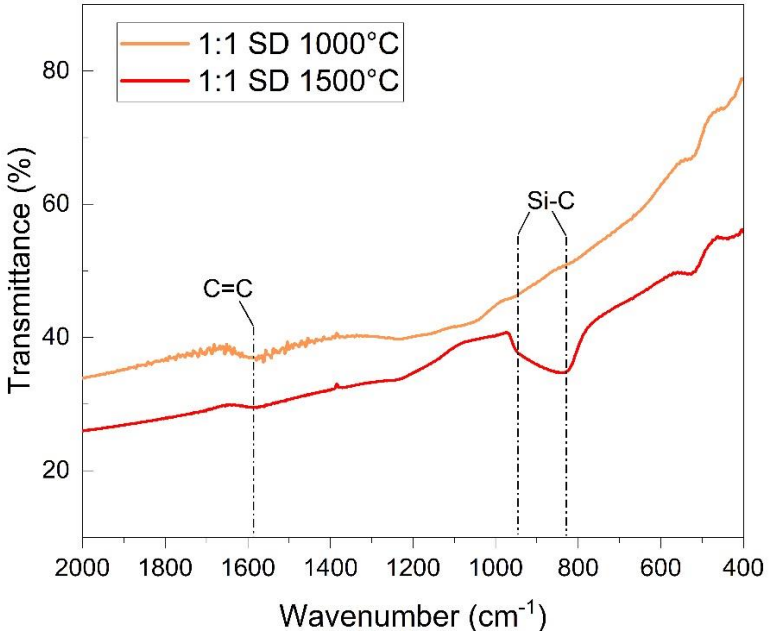

Figure 2: Infrared spectra of the ceramic aerogels pyrolyzed at 1000°C and 1500°C. Acquired in transmission.

As ceramization occurs, a certain level of shrinkage of the porous structure is known to happen, as depicted by the N_2 physisorption analysis reported in **Figure 3a,b**. When pyrolyzed at 1000°C, the aerogel loses porosity along the whole pore size range, especially on fraction of small mesopores with diameter < 10 nm (inset in **Figure 3a**), resulting in a SSA of 102 $m^2 \cdot g^{-1}$ and a pore volume of 0.68 $cm^3 \cdot g^{-1}$. On the other hand, the pore size distribution of the aerogel treated at 1500°C shifts to the micro-mesopore range partially re-gaining small mesopores giving a pore volume of 0.47 $cm^3 \cdot g^{-1}$. Multipoint BET calculations indicate a specific surface area of 215 $m^2 \cdot g^{-1}$. The isotherm shows a plateau near the saturation point, which is consistent with the mesoporous distribution, and it can be addressed as a Type IV isotherm with a H1 hysteresis shape [25]. Such type of hysteresis is indeed typical of narrow pores distributions, and in the present case it is possibly given by the predominant fraction of pores with a diameter around 30 nm, as suggested by the steep section of the cumulative pore volume curve (inset in **Figure 3b**). The evolution of porosity as described above occurs as a consequence of crystallization and phase separation between SiC and free carbon domains, as discussed in the following section.

Figure 3c shows the N_2 physisorption isotherm and the QSDFT pore size distributions of activated carbon available at the municipal drinking water plant of the city of Turin. Given its nature, it results highly microporous, with most of the pore volume contained by cavities smaller than 2 nm. As a matter of fact, the isotherm shape can be classified as Type I, with an extremely large SSA of 1073 $m^2 \cdot g^{-1}$ and a pore volume of 0.44 $cm^3 \cdot g^{-1}$. All results are tabulated in **Table 1**.

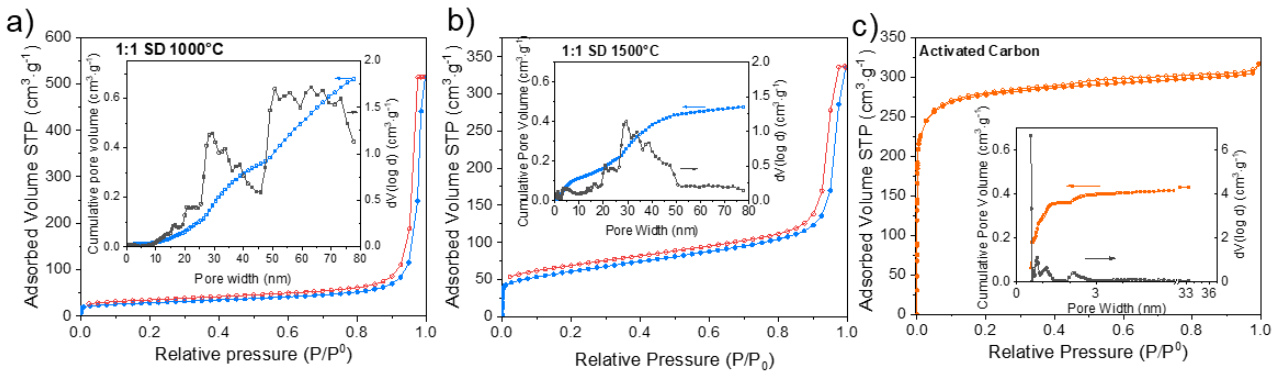

Figure 3: N_2 Adsorption/desorption isotherm and DFT pore volume distribution (inset) of the tested sorbents: a) 1:1 SD pyrolyzed at 1000°C; b) 1:1 SD pyrolyzed at 1500°C; c) Activated carbon.

Table 1: Specific surface areas and DFT pore volumes of the tested sorbents: a) 1:1 SD 1000°C; b) 1:1 SD 1500°C; c) Activated carbons

Specimen	1:1 SD 1000°C	1:1 SD 1500°C	Activated Carbon
SSA ($m^2 \cdot g^{-1}$)	102	215	1073
Pore Vol ($cm^3 \cdot g^{-1}$)	0.68	0.47	0.44

The morphology of the ceramic aerogel at 1500 °C can be observed in **Figure 4 a,b**. Crystals with dimensions of 100-200 nm are dispersed in the porous colloidal matrix. According to the acquired XRD pattern in **Figure 5a**, these crystals correspond to cubic β-SiC (JCPDS: 29-1129), as expected from the pyrolysis of a polycarbosilane. In particular, the maximum peak intensity found at $2\theta = 41.7°$ corresponds to the (111) crystal plane of β-SiC. A shoulder peak arising at $2\theta = 39.1°$ can be assigned to stacking faults of the β-SiC structure [29]. Therefore, the non-crystalline microstructure can be considered to be mainly composed of amorphous silicon carbide and free carbon.

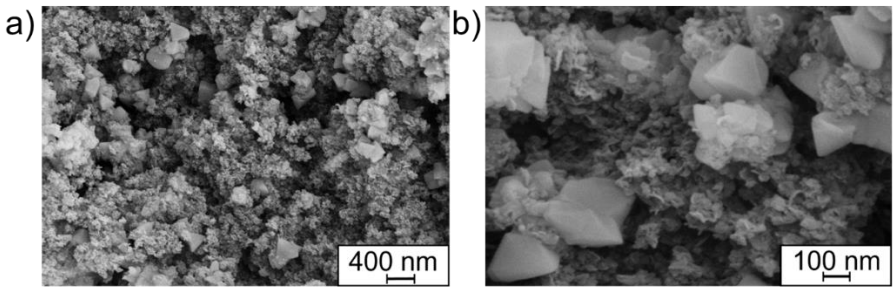

Figure 4: a), b): SEM acquisitions on the ceramic aerogel(pyrolyzed at 1500°C in argon) featuring nanosized crystals.

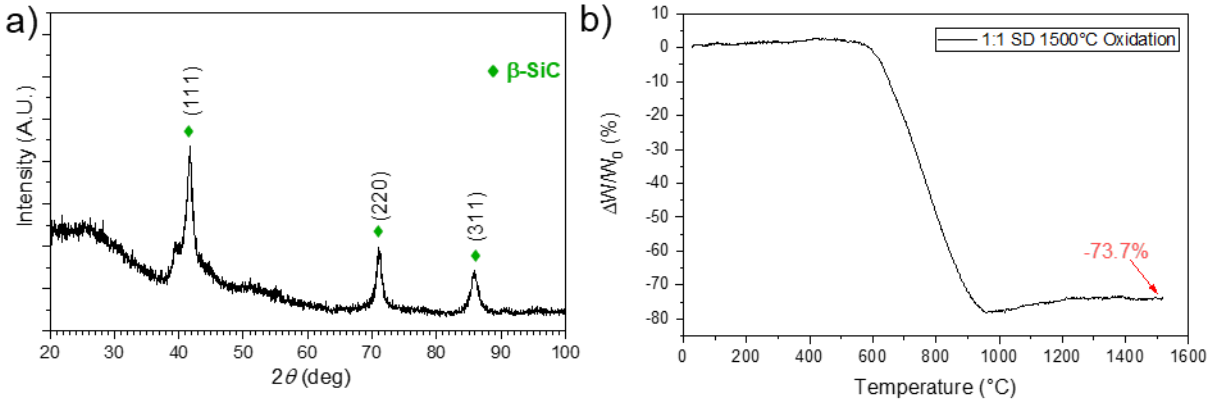

Figure 5: a) XRD pattern of the aerogel pyrolyzed at 1500°C showing the presence of beta silicon carbide; b) Weight evolution of ceramic aerogel under fluxed air, thermogravimetric analysis.

In order to roughly assess the weight fractions of free carbon and silicon carbide, an oxidative thermogravimetric analysis was performed. In principle, carbon is expected to oxidize and volatilize under the form of CO_2 starting from 450-500°C, while the oxidation of SiC takes place from 900°C, generating SiO_2 [11]. Thus, knowing the amount of residual mass and assuming that only pure silica is left, it is possible to give a rough estimate of the amount of the two initial components. Results are given in **Figure 5b**, from which a weight fraction of 17.5% SiC was calculated (the remaining 82.5% is free carbon).

3.2 Adsorption performance

Preliminary adsorption tests performed on aerogel ceramized at 1000°C and 1500 °C indicated a low removal performance (13%) for the aerogel treated at 1000 °C and a quantitative removal for the aerogel obtained at 1500 °C (time of contact 48h).

For its higher removal performance, the aerogel obtained at 1500 °C was further studied through adsorption kinetics and isotherms.

3.2.1 Adsorption kinetics

The adsorption kinetic profile of the ceramic aerogel (1500 °C) towards glyphosate was studied to find best non-irreversible equilibrium conditions at which isotherm tests could be performed. The resulting glyphosate adsorption (R_{ads}%) as a function of contact time (t) is given in **Figure 6**.

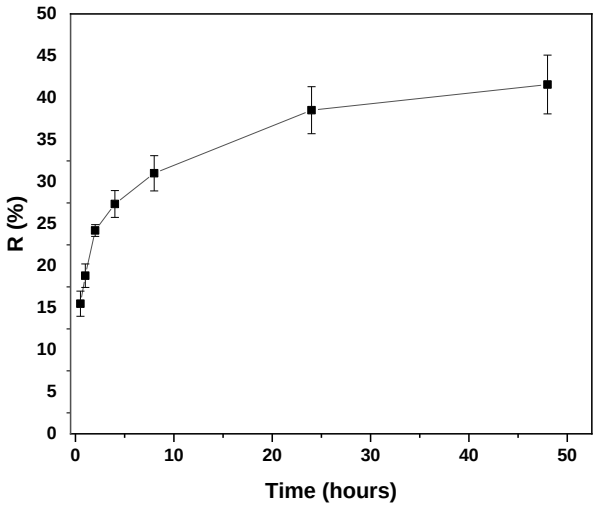

Figure 6: Glyphosate adsorption (R_{ads}%) on 0.025 g the ceramic aerogel (1500°C) as a function of contact time. Deviation bars are also reported.

Adsorption equilibrium is shown to be achieved after 24 hours contact time at non-irreversible conditions (38.5±1.8% of glyphosate retained from the solution), being compatible for further adsorption isotherm studies (see paragraph 3.2.2). In addition, the adsorption kinetic trend increases over time, thus suggesting that no competitive adsorption with water molecules occurred on active sites as elsewhere observed for more hydrophilic substrates of similar SSA and mesoporosity [30].

To quantitatively analyse the kinetics of glyphosate adsorption, experimental data were fitted by employing pseudo-first-order, pseudo-second order and Elovich equations (Eq. 3,4,5), hereafter reported in their linearized form:

$$Pseudo - first\ order: \ln(q_e - q_t) = \ln(q_e) - k_1 t \quad (3)$$

$$Pseudo - second\ order: \frac{t}{q_t} = \frac{1}{k_2 q_e^2} + \frac{t}{q_e} \quad (4)$$

$$Elovich: q_t = \frac{1}{\beta}\ln(\alpha\beta) + \frac{1}{\beta}\ln(t) \quad (5)$$

where *i)* q_t and q_e represent the adsorption capacities ($\mu g \cdot g^{-1}$) at contact time t (expressed as hours) and at the equilibrium, respectively; *ii)* k_1 and k_2 are the rate constants of the pseudo-first and pseudo-second models; *iii)* α and β are the initial adsorption rate ($\mu g \cdot g^{-1}$ $hour^{-1}$) and the desorption rate ($g \cdot \mu g^{-1}$) of the Elovich model, respectively. For each of the above-mentioned model, fitting equations and R^2 values were determined (**Table 2**).

Table 2: Modelling of glyphosate kinetic adsorption data on the ceramic aerogel

	Linearized fitting equation	**R^2**	**Parameters**
Pseudo-first order	$ln(q_e\text{-}q_t) = 329.4 - 0.1t$	0.987	q_e = 329.4 $\mu g \cdot g^{-1}$ k_1 = 0.23 min^{-1}
Pseudo-second order	$t/q_t = 1.6 \cdot 10^{-3} + t/594.8$	0.998	q_e = 594.8 $\mu g \cdot g^{-1}$ k_2 = $1.1 \cdot 10^{-3}$ $g \cdot \mu g^{-1}$ min^{-1} h = 336.5 $\mu g \cdot g^{-1}$ min^{-1}
Elovich	$q_t = 274 + 200\ ln(t)$	0.992	α = 788.6 $\mu g \cdot g^{-1}$ min^{-1} β = $5.3 \cdot 10^{-3}$ $g \cdot \mu g^{-1}$

R^2 values do not clearly state which of the tested models is the most suitable to describe the adsorption of glyphosate on the ceramic aerogel. Hence, the kinetic parameters obtained for each model were used to recalculate the adsorption qt values; the percentage error ($\%_{error}$) between calculated and experimental q_t

($\%_{error} = \left|\frac{q_{t\ calculated} - q_{t\ experimental}}{q_{t\ calculated}}\right| * 100$) was chosen as discriminant parameter to evaluate the best model. Average $\%_{errors}$ were 68.5% for q_t calculated with pseudo-first order model, 12.6% for pseudo-second order and 2.8% for Elovich. Such results clearly show that glyphosate adsorbed from the ceramic aerogel follows the Elovich kinetic equation, thus assuming that the rate of adsorption exponentially decreases with the increase in amount of glyphosate adsorbed onto the ceramic aerogel surface without any interaction among the adsorbed species [31]. Experimental and calculated values of adsorption kinetics for glyphosate on ceramic aerogel according to linearized Elovich model are reported in **Figure 7**.

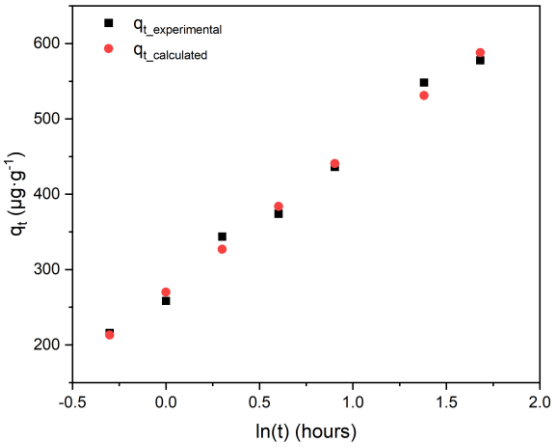

Figure 7: Linearization of Elovich model for the adsorption of glyphosate on the ceramic aerogel, experimental (black squares) and calculated (red dots) values.

3.2.2 Adsorption isotherm

In order to choose the proper mass range to be used in the experimental set-up for the adsorption isotherm tests, preliminary adsorption tests were performed at 24 h contact time using 0.05 g and 0.1 g of the aerogel, obtaining adsorption fractions of 68.5 ± 4.0 and quantitative adsorption, respectively. Hence the mass range was kept below 0.1 g.

The adsorption isotherm at room temperature is shown in **Figure 8**, whereas values of adsorbed amount q_e ($mg \cdot g^{-1}$) and equilibrium concentration C_e ($mg \cdot L^{-1}$) are listed in **Table 3**, together with initial aerogel mass

(g) and corresponding removal percentage (R_{ads}). Data show that adsorption percentage increases with the increase of the adsorbent mass and, in turn, decreases with the increase of residual glyphosate concentration. Following Giles indications, the adsorption isotherm obtained plotting q_e as a function of residual glyphosate concentration appears as L- or H- type [32]. Hence, the obtained experimental data were fitted with the three models hereafter described:

– The Langmuir model ([33]), which is shown in the linearized form in **Equation 6**. It describes the formation of a monolayer of adsorbate under the assumptions that: *i)* the surface is homogeneous and constituted of identical binding sites; *ii)* the sites are independent (no interaction between adsorbed molecules); and *iii)* each site on the surface can hold at most one molecule of adsorbate.

$$\frac{C_e}{q_e} = \frac{1}{K_L \cdot Q_0} + \frac{C_e}{Q_0} \tag{6}$$

Here, K_L is the adsorption equilibrium constant ($L \cdot mg^{-1}$) and Q_0 is the maximum monolayer coverage capacity ($mg \cdot g^{-1}$).

– The Freundlich isotherm, linearized in **Equation 7** [34][35], is the most applied empirical model to describe a non-ideal and reversible adsorption; it is not limited to the formation of a monolayer but accounts for multilayer adsorption in heterogeneous systems:

$$\ln(q_e) = \ln(K_F) + \frac{1}{n}\ln(C_e) \tag{7}$$

where K_F ($mg^{1-1/n}\, L^{1/n} \cdot g^{-1}$) is the adsorption coefficient, *1/n* is a measure of surface heterogeneity

– The Temkin ([36]) model, **Equation 8**, which postulates that the heat of adsorption varies linearly with coverage, unlike the Freundlich method, which assumes a more complex dependence of the heat of adsorption on the coverage (i.e., the heat of adsorption decreases exponentially with increasing coverage):

$$q_e = a + b\ln(C_e \cdot q_e) \tag{8}$$

where *a* and *b* are empirical constants.

Among the three models, the Langmuir one showed the best R^2 value (i.e., R^2=0.9987 – Langmuir; R^2= 0.9299 – Freundlich; R^2=0.9309 – Temkin).

The isotherm calculated using the above-mentioned parameters showed a very good agreement with the experimental one (**Figure 6**). Since the best fitting was obtained with the Langmuir model, we propose that the experimental adsorption isotherm is of the L-Type, according to the classification reported by Giles.

The Langmuir capacity was calculated by fitting the adsorption data, obtaining a value of 0.607 mg·g^{-1}.

The Langmuir isotherm allowed to determine the value of the dimensionless separation parameter, R_L, in order to define whether the aerogel system provides favourable or unfavourable adsorption. R_L was calculated using **Equation 9** [37]:

$$R_L = \frac{1}{1 + K_L \cdot C_0} \quad (9)$$

where K_L is the Langmuir isotherm constant and C_0 is the initial concentration of glyphosate (mg·L^{-1}). The shapes of the isotherm for $0 < R_L < 1$, $R_L > 1$, $R_L = 1$, and $R_L = 0$ indicate favourable, unfavourable, linear and irreversible adsorption, respectively [38,39]. The R_L at room temperature was 0.02, indicating very favourable adsorption.

Finally, the change in free energy (ΔG^0) was calculated according to **Equation 10**:

$$\Delta G^0 = RT \ln(K^0) \quad (10)$$

where R is the universal gas constant (8.314 J mol^{-1}·K^{-1}), T (K) is the absolute temperature (298 K), $K°$= K_L (L·mg^{-1})·molecular weight of glyphosate (169.07 g·mol^{-1})·10^3·55.5 mol·L^{-1} [40]The negative value of ΔG^0 for glyphosate-aerogel system (− 47.5 kJ·mol^{-1}), confirms that the adsorption reaction is thermodynamically favoured.

Table 3: Adsorption parameters of glyphosate onto the aerogel surface as a function of the aerogel mass.

m (g)	R_{ads} (%)	C_e (mg·L^{-1})	q_e (mg·g^{-1})
0.02522	41.3	1.175	0.575

0.03005	50.1	0.997	0.592
0.04062	66.7	0.667	0.580
0.04987	77.8	0.445	0.547
0.06116	87.2	0.256	0.500
0.07077	93.2	0.136	0.462

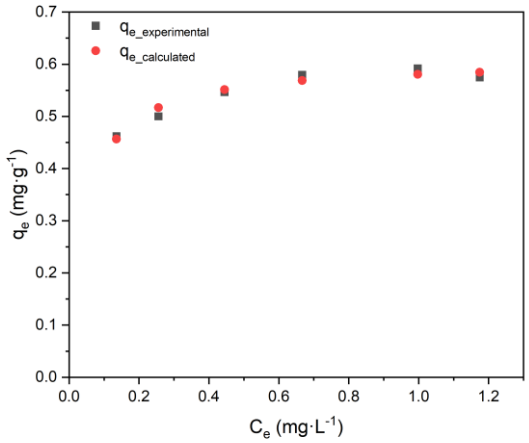

Figure 8: Adsorption isotherm of glyphosate onto aerogel. Experimental (black squares) and calculated (red dots) values according to the Langmuir model (K_L=22.5 L·mol^{-1}). Experimental conditions: variable mass of aerogel (range 0.0053-0.071 g) in contact with 17 mL of glyphosate solution

The adsorption data of the aerogel ceramized at 1500 °C were compared with adsorption data on glyphosate (C_e, q_e) available at the municipal drinking water plant of the city of Turin conducted on the activated carbon, here characterized for the purpose (SSA: 1073 m^2·g^{-1}; pore volume 0.44 cm^3·g^{-1}). Comparing the adsorption data of the activated carbon with those calculated for the aerogel using the parameters obtained by the Langmuir isotherm, it is possible to obtain q_e values for the aerogel of one order of magnitude higher than those obtained with activated carbon, for instance, 0.52 vs 0.014 mg g^{-1} and 0.55 vs 0.055 mg g^{-1}. Even if this comparison derives from an approximation approach, this result is a strong indication of the better adsorptive performance of the aerogel with respect to activated carbon.

4. Conclusions

The polycarbosilane-derived silicon carbide aerogel here prepared is a suitable sorbent for glyphosate capture from water. Adsorption equilibrium is achieved within 24 h, following the Elovich's kinetic model. According to the Langmuir model, which represents the best fit of the experimental adsorption isotherm data, the adsorption capacity is 0.607 $mg \cdot g^{-1}$. A comparison with extrapolated q_e for the aerogel with experimental q_e available for activated carbon used in the potabilization plant, allows to hypothesize better adsorptive performances of the aerogel with respect to activated carbons. This results confirms that Polymer Derived Ceramic aerogels are suitable materials for developing adsorbers for water purification. However, more effort is needed to explain the high affinity of the studied SiC/C aerogels towards glyphosate adsorption.

Acknowledgements

Andrea Zambotti, Maria Concetta Bruzzoniti and Gian Domenico Sorarù greatly acknowledge the financial support by the Italian Ministry of University and Research (MIUR) within the program PRIN2017 - 2017PMR932 "Nanostructured Porous Ceramics for Environmental and Energy Applications". The authors acknowledge Mr. E. Cagno, for his laboratory assistance.

References

1. Özkara, A.; Akyil, D.; Konuk, M. Pesticides, Environmental Pollution, and Health. *Environ. Heal. Risk - Hazard. Factors to Living Species* **2016**, 3–28, doi:10.5772/63094.

2. Verger, P.J.P.; Boobis, A.R. Reevaluate pesticides for food security and safety. *Science (80-.).* **2013**, *341*, 717–718, doi:10.1126/science.1241572.

3. Weichenthal, S.; Moase, C.; Chan, P. A review of pesticide exposure and cancer incidence in the agricultural health study cohort. *Environ. Health Perspect.* **2010**, *118*, 1117–1125, doi:10.1289/ehp.0901731.

4. Martin, F.L.; Martinez, E.Z.; Stopper, H.; Garcia, S.B.; Uyemura, S.A.; Kannen, V. Increased exposure to pesticides and colon cancer: Early evidence in Brazil. *Chemosphere* **2018**, *209*, 623–631, doi:10.1016/j.chemosphere.2018.06.118.

5. Malone, R.W.; Ahuja, L.R.; Ma, L.; Wauchope, R.D.; Ma, Q.; Rojas, K.W. Application of the Root Zone Water Quality Model (RZWQM), to pesticide fate and transport: An overview. *Pest Manag. Sci.* **2004**, *60*, 205–221, doi:10.1002/ps.789.

6. Nguyen, D.C.; Vezentsev, A.I.; Sokolovskiy, P. V.; Greish, A.A. Adsorption of Glyphosate on Carbon-Containing Materials. *Russ. J. Phys. Chem. A* **2021**, *95*, 1212–1215, doi:10.1134/S0036024421060194.

7. Diel, J.C.; Franco, D.S.P.; Nunes, I.D.S.; Pereira, H.A.; Moreira, K.S.; Thiago, T.A.; Foletto, E.L.; Dotto, G.L. Carbon nanotubes impregnated with metallic nanoparticles and their application as an adsorbent for the glyphosate removal in an aqueous matrix. *J. Environ. Chem. Eng.* **2021**, *9*, doi:10.1016/j.jece.2021.105178.

8. Soares, S.F.; Amorim, C.O.; Amaral, J.S.; Trindade, T.; Daniel-Da-Silva, A.L. On the efficient removal, regeneration and reuse of quaternary chitosan magnetite nanosorbents for glyphosate herbicide in water. *J. Environ. Chem. Eng.* **2021**, *9*, doi:10.1016/j.jece.2021.105189.

9. Pereira, H.A.; Hernandes, P.R.T.; Netto, M.S.; Reske, G.D.; Vieceli, V.; Oliveira, L.F.S.; Dotto, G.L. Adsorbents for glyphosate removal in contaminated waters: a review. *Environ. Chem. Lett.* **2021**, *19*, 1525–1543, doi:10.1007/s10311-020-01108-4.

10. Colombo, P.; Mera, G.; Riedel, R.; Sorarù, G.D. Polymer-derived ceramics: 40 Years of research and innovation in advanced ceramics. *J. Am. Ceram. Soc.* **2010**, *93*, 1805–1837, doi:10.1111/j.1551-2916.2010.03876.x.

11. Sorarù, G.D.; Zera, E.; Campostrini, R. Aerogels from preceramic Polymers. In *Handbook of Sol-Gel Science and Technology*; 2017 ISBN 9783319194547.

12. Zambotti, A.; Caldesi, E.; Pellizzari, M.; Valentini, F.; Pegoretti, A.; Dorigato, A.; Speranza, G.; Chen, K.; Bortolotti, M.; Sorarù, G.D.; et al. Polymer-derived silicon nitride aerogels as shape stabilizers for low and high-temperature thermal energy storage. *J. Eur. Ceram. Soc.* **2021**, *41*, 5484–5494,

doi:10.1016/j.jeurceramsoc.2021.04.056.

13. Zambotti, A.; Valentini, F.; Lodi, E.; Pegoretti, A.; Tyrpekl, V.; Kohúteková, S.; Sorarù, G.D.; Kloda, M.; Biesuz, M. Thermochemical heat storage performances of magnesium sulphate confined in polymer-derived SiOC aerogels. *J. Alloys Compd.* **2022**, *895*, doi:10.1016/j.jallcom.2021.162592.

14. Vakifahmetoglu, C.; Semerci, T.; Gurlo, A.; Soraru, G.D. Polymer derived ceramic aerogels. *Curr. Opin. Solid State Mater. Sci.* **2021**, *25*, 100936, doi:10.1016/j.cossms.2021.100936.

15. Pradeep, V.S.; Ayana, D.G.; Graczyk-Zajac, M.; Soraru, G.D.; Riedel, R. High Rate Capability of SiOC Ceramic Aerogels with Tailored Porosity as Anode Materials for Li-ion Batteries. *Electrochim. Acta* **2015**, *157*, 41–45, doi:10.1016/j.electacta.2015.01.088.

16. Icin, O.; Vakifahmetoglu, C. Dye removal by polymer derived ceramic nanobeads. *Ceram. Int.* **2021**, *47*, 27050–27057, doi:10.1016/j.ceramint.2021.06.118.

17. Bruzzoniti, M.C.; Appendini, M.; Onida, B.; Castiglioni, M.; Del Bubba, M.; Vanzetti, L.; Jana, P.; Sorarù, G.D.; Rivoira, L. Regenerable, innovative porous silicon-based polymer-derived ceramics for removal of methylene blue and rhodamine B from textile and environmental waters. *Environ. Sci. Pollut. Res.* **2018**, *25*, 10619–10629, doi:10.1007/s11356-018-1367-x.

18. Jana, P.; Bruzzoniti, M.C.; Appendini, M.; Rivoira, L.; Del Bubba, M.; Rossini, D.; Ciofi, L.; Sorarù, G.D. Processing of polymer-derived silicon carbide foams and their adsorption capacity for non-steroidal anti-inflammatory drugs. *Ceram. Int.* **2016**, *42*, 18937–18943, doi:10.1016/j.ceramint.2016.09.045.

19. Zera, E.; Brancaccio, E.; Tognana, L.; Rivoira, L.; Bruzzoniti, M.C.; Sorarù, G.D. Reactive Atmosphere Synthesis of Polymer-Derived Si–O–C–N Aerogels and Their Cr Adsorption from Aqueous Solutions. *Adv. Eng. Mater.* **2018**, *20*, 1–9, doi:10.1002/adem.201701130.

20. Zera, E.; Campostrini, R.; Aravind, P.R.; Blum, Y.; Sorarù, G.D. Novel SiC/C aerogels through pyrolysis of polycarbosilane precursors. *Adv. Eng. Mater.* **2014**, *16*, 814–819, doi:10.1002/adem.201400134.

21. Li, H.; Zhang, L.; Cheng, L.; Wang, Y.; Yu, Z.; Huang, M.; Tu, H.; Xia, H. Polymer-ceramic conversion of a highly branched liquid polycarbosilane for SiC-based ceramics. *J. Mater. Sci.* **2008**, *43*, 2806–2811, doi:10.1007/s10853-008-2539-8.

22. Dalcanale, F.; Grossenbacher, J.; Blugan, G.; Gullo, M.R.; Lauria, A.; Brugger, J.; Tevaearai, H.; Graule, T.; Niederberger, M.; Kuebler, J. Influence of carbon enrichment on electrical conductivity and processing of polycarbosilane derived ceramic for MEMS applications. *J. Eur. Ceram. Soc.* **2014**, *34*, 3559–3570, doi:10.1016/j.jeurceramsoc.2014.06.002.

23. Kaur, S.; Riedel, R.; Ionescu, E. Pressureless fabrication of dense monolithic SiC ceramics from a polycarbosilane. *J. Eur. Ceram. Soc.* **2014**, *34*, 3571–3578, doi:10.1016/j.jeurceramsoc.2014.05.002.

24. Laine, R.M.; Babonneau, F. Preceramic Polymer Routes to Silicon Carbide. *Chem. Mater.* **1993**, *5*, 260–279, doi:10.1021/cm00027a007.

25. Rouquerol, F.; Rouquerol, J.; Sing, K.S.W.; Llewellyn, P.; Maurin, G. *Adsorption by Powders and Porous Solids*; 2014; ISBN 9780080970356.

26. Pitman, K.M.; Hofmeister, A.M.; Corman, A.B.; Speck, A.K. Optical properties of silicon carbide for astrophysical applications. *Astron. Astrophys.* **2008**, *483*, 661–672, doi:10.1051/0004-6361:20078468.

27. Hofmeister, A.M.; Pitman, K.M.; Goncharov, A.F.; Speck, A.K. Optical constants of silicon carbide for astrophysical applications. II. Extending optical functions from infrared to ultraviolet using single-crystal absorption spectra. *Astrophys. J.* **2009**, *696*, 1502–1516, doi:10.1088/0004-637X/696/2/1502.

28. Assefa, D.; Zera, E.; Campostrini, R.; Soraru, G.D.; Vakifahmetoglu, C. Polymer-derived SiOC aerogel with hierarchical porosity through HF etching. *Ceram. Int.* **2016**, *42*, 11805–11809, doi:10.1016/j.ceramint.2016.04.101.

29. Liu, Y.; Hou, H.; He, X.; Yang, W. Mesporous 3C-SiC Hollow Fibers. *Sci. Rep.* **2017**, *7*, 1–8, doi:10.1038/s41598-017-02147-8.

30. Bruzzoniti, M.C.; De Carlo, R.M.; Rivoira, L.; Del Bubba, M.; Pavani, M.; Riatti, M.; Onida, B. Adsorption of bentazone herbicide onto mesoporous silica: application to environmental water

purification. *Environ. Sci. Pollut. Res.* **2016**, *23*, 5399–5409, doi:10.1007/s11356-015-5755-1.

31. Wu, F.C.; Tseng, R.L.; Juang, R.S. Characteristics of Elovich equation used for the analysis of adsorption kinetics in dye-chitosan systems. *Chem. Eng. J.* **2009**, *150*, 366–373, doi:10.1016/j.cej.2009.01.014.

32. Giles, C.H.; MacEwan, T.H.; Nakhwa, S.N.; Smith, D. 786. Studies in adsorption. Part XI. A system of classification of solution adsorption isotherms, and its use in diagnosis of adsorption mechanisms and in measurement of specific surface areas of solids. *J. Chem. Soc.* **1960**, *846*, 3973, doi:10.1039/jr9600003973.

33. Liu, Y. Some consideration on the Langmuir isotherm equation. *Colloids Surfaces A Physicochem. Eng. Asp.* **2006**, *274*, 34–36, doi:10.1016/j.colsurfa.2005.08.029.

34. Freundlich, H.M.F. Over the adsorption in solution. *J. Phys. chem.* **1906**, *57*, 1100–1107.

35. Foo, K.Y.; Hameed, B.H. Insights into the modeling of adsorption isotherm systems. *Chem. Eng. J.* **2010**, *156*, 2–10, doi:10.1016/j.cej.2009.09.013.

36. Temkin, M.; Pyzhev, V. Kinetics of ammonia synthesis on promoted iron catalyst. *Acta Phys. Chim.* **1940**, *12*, 327–356.

37. Weber, T.W.; Chakravorti, R.K. Pore and solid diffusion models for fixed-bed adsorbers. *AIChE J.* **1974**, *20*, 228–238, doi:10.1002/aic.690200204.

38. Vasanth Kumar, K.; Sivanesan, S. Isotherms for Malachite Green onto rubber wood (Hevea brasiliensis) sawdust: Comparison of linear and non-linear methods. *Dye. Pigment.* **2007**, *72*, 124–129, doi:10.1016/j.dyepig.2005.07.021.

39. Piccolo, A.; Celano, G.; Arienzo, M.; Mirabella, A. Adsorption and desorption of glyphosate in some European soils. *J. Environ. Sci. Heal. Part B* **1994**, *29*, 1105–1115, doi:10.1080/03601239409372918.

40. Zhou, X.; Zhou, X. the Unit Problem in the Thermodynamic Calculation of Adsorption Using the Langmuir Equation. *Chem. Eng. Commun.* **2014**, *201*, 1459–1467, doi:10.1080/00986445.2013.818541.